Insect Biochemistry and Molecular Biology 138 (2021) 103647

Contents lists available at ScienceDirect

Insect Biochemistry and Molecular Biology

journal homepage: www.elsevier.com/locate/ibmb

The cytochrome P450 *CYP325A* is a major driver of pyrethroid resistance in the major malaria vector *Anopheles funestus* in Central Africa

Amelie N.R. Wamba [a,b,*], Sulaiman S. Ibrahim [c,d], Michael O. Kusimo [a], Abdullahi Muhammad [c,g], Leon M.J. Mugenzi [a,f], Helen Irving [c], Murielle J. Wondji [a,c], Jack Hearn [c], Jude D. Bigoga [c,e], Charles S. Wondji [a,c,**]

[a] *Centre for Research in Infectious Diseases (CRID), P.O. BOX 13591, Yaoundé, Cameroon*
[b] *Faculty of Science, Department of Biochemistry, University of Yaoundé I, P.O. Box 812, Yaoundé, Cameroon*
[c] *Vector Biology Department, Liverpool School of Tropical Medicine (LSTM), Pembroke Place, Liverpool, L3 5QA, UK*
[d] *Department of Biochemistry, Bayero University, PMB, 3011, Kano, Nigeria*
[e] *Laboratory for Vector Biology and Control, National Reference Unit for Vector Control, The Biotechnology Centre, Nkolbisson – University of Yaoundé I, P.O. Box 3851, Messa, Yaoundé, Cameroon*
[f] *Department of Biochemistry and Molecular Biology, Faculty of Science, University of Buea, P.O. Box 63, Buea, Cameroon*
[g] *Centre for Biotechnology Research, Bayero University, Kano, PMB, 3011, Kano Nigeria*

ARTICLE INFO

Keywords:
Anopheles funestus
Malaria
Pyrethroids
Metabolic resistance
Cytochrome P450– *CYP325A*
Central Africa

ABSTRACT

The overexpression and overactivity of key cytochrome P450s (CYP450) genes are major drivers of metabolic resistance to insecticides in African malaria vectors such as *Anopheles funestus* s.s. Previous RNAseq-based transcription analyses revealed elevated expression of *CYP325A* specific to Central African populations but its role in conferring resistance has not previously been demonstrated. In this study, RT-qPCR consistently confirmed that *CYP325A* is highly over-expressed in pyrethroid-resistant *An. funestus* from Cameroon, compared with a control strain and insecticide-unexposed mosquitoes. A synergist bioassay with PBO significantly recovered susceptibility for permethrin and deltamethrin indicating P450-based metabolic resistance. Analyses of the coding sequence of *CYP325A* Africa-wide detected high-levels of polymorphism, but with no predominant alleles selected by pyrethroid resistance. Geographical amino acid changes were detected notably in Cameroon. *In silico* homology modelling and molecular docking simulations predicted that *CYP325A* binds and metabolises type I and type II pyrethroids. Heterologous expression of recombinant CYP325A and metabolic assays confirmed that the most-common Cameroonian haplotype metabolises both type I and type II pyrethroids with depletion rate twice that the of the DR Congo haplotype. Analysis of the 1 kb putative promoter of *CYP325A* revealed reduced diversity in resistant mosquitoes compared to susceptible ones, suggesting a potential selective sweep in this region. The establishment of *CYP325A* as a pyrethroid resistance metabolising gene further explains pyrethroid resistance in Central African populations of *An. funestus*. Our work will facilitate future efforts to detect the causative resistance markers in the promoter region of *CYP325A* to design field applicable DNA-based diagnostic tools.

1. Introduction

Malaria remains a major cause of death in Africa which shoulders about 94% of the global burden with 229 million malaria cases and 409,000 deaths recorded worldwide in 2019, mostly among pregnant women and children under five years of age (WHO, 2020). Cameroon bears approximately 3% of this global burden accounting for 23.6% of consultations in health centres, 68.7% of deaths in children below five years and 16.9% of deaths in pregnant women (Diengou et al., 2020; Tonye et al., 2018). Major vectors of malaria across Africa and in

* Corresponding author. Centre for Research in Infectious Diseases (CRID), P.O. BOX 13591, Yaoundé, Cameroon.
** Corresponding author. Vector Biology Department, Liverpool School of Tropical Medicine (LSTM), Pembroke Place, Liverpool, L3 5QA, UK.
E-mail addresses: amelie.wamba@crid-cam.net (A.N.R. Wamba), charles.wondji@lstmed.ac.uk (S.S. Ibrahim), gkusimo@gmail.com (M.O. Kusimo), abdullahi.muhammad@lstmed.ac.uk (A. Muhammad), leon.mugenzi@crid-cam.net (L.M.J. Mugenzi), helen.irving@lstmed.ac.uk (H. Irving), murielle.wondji@lstmed.ac.uk (M.J. Wondji), jack.hearn@lstmed.ac.uk (J. Hearn), judebigoga@yahoo.com (J.D. Bigoga), charles.wondji@lstmed.ac.uk (C.S. Wondji).

https://doi.org/10.1016/j.ibmb.2021.103647
Received 15 July 2021; Received in revised form 20 August 2021; Accepted 7 September 2021
Available online 14 September 2021

Cameroon are *An. gambiae s.l.* and *An. funestus,* which are both widely distributed (Antonio-Nkondjio et al., 2012), have high vector competences for *Plasmodium*, are highly anthropophilic (Tchuinkam et al., 2015) and thrive in urban and rural environments (Djouaka et al., 2016). The relative abundance of these vectors due to favourable climatic conditions and abundant breeding sites, is directly linked to malaria incidence rates in endemic areas and therefore a major public health concern (Antonio-Nkondjio et al., 2011).

Malaria prevention relies heavily on the use of insecticide-based interventions such as long lasting insecticidal nets (LLINs) and IRS (Indoor Residual Spraying) (Mendis et al., 2009). Pyrethroids remain the most widely used and main class of insecticides recommended by WHO for adult vector control through bed net treatment and IRS (WHO, 2020). However an alarmingly rapid increase and spread of pyrethroid resistance in malaria vectors *An. gambiae* and *An. funestus* poses a huge threat to the continued efficacy of current pyrethroid-based interventions (Riveron et al., 2013).

The two major mechanisms of insecticide resistance in mosquitoes are target-site resistance in the voltage-gated sodium channel (*kdr*) and metabolic resistance (Riveron et al., 2018a). Cytochrome P450 monooxygenase (CYP)-mediated detoxification is a major mechanism driving pyrethroid resistance in mosquitoes (Riveron et al., 2016), more so, in *An. funestus* where there is currently no evidence of target-site resistance (*kdr*) implying the resistance mechanism is principally metabolic (Hemingway, 2014; Moyes et al., 2020). Several studies already confirmed through QTL mapping and other analyses, the role of CYP6 cluster genes in *An. funestus* (Wondji et al., 2007) and *An. gambiae* (Nikou et al., 2003) pyrethroid-based resistance. Genome-wide transcriptomic analyses have implicated many over-expressed CYP450s in metabolic resistance in *An. funestus* across Africa (Riveron et al., 2017). The over-expression of these P450s has been characterised by a regional split as specific genes are over-expressed in different regions (Riveron et al., 2017; Weedall et al., 2019). This is supported by the massive over-expression of *CYP6P9a/b* duplicated genes in southern Africa which does not occur in other regions. Recent progress has led to extensive characterisation of the *CYP6P9a/b* driven resistance with detection of DNA-based markers driving this resistance (Mugenzi et al., 2019; Weedall et al., 2019) allowing the use of PCR-based assays to detect such resistance in individual mosquitoes. However, separate assays must be designed for other regions such as Central Africa where different genes have been shown to be over-expressed. Among CYP450s, *CYP325A* has been shown to have the greatest fold change among P450s in the Central Africa region versus a susceptible strain of *An. funestus* (Mugenzi et al., 2019; Weedall et al., 2020). Several studies have characterised the role of *Anopheles* CYP450s in insecticide resistance, using *in silico* homology modelling/substrate docking, in addition to heterologous expression of recombinant CYP450s and activity assays. For example, *CYP6P3* and *CYP6M2* shown to confer pyrethroid resistance in *Anopheles gambiae* (Müller et al., 2008; Stevenson, B. et al., 2011; Stevenson, Bradley J et al., 2011) and *CYP6Z1* shown to metabolise DDT in the same species (Chiu et al., 2008). In *An. funestus* previous study has used docking and activity assays to establish allelic variation impacting pyrethroid resistance in the resistance genes, *CYP6P9a* and *CYP6P9b* (Ibrahim et al., 2015) as well as the role of the *CYP6Z1* in cross-resistance to pyrethroid and bendiocarb (Ibrahim et al., 2016a). Also, *in silico* analysis of the 5′UTR regulatory element of the major *An. funestus* pyrethroid resistance gene *CYP6P9a*, coupled with promoter activity assay (dual luciferase reporter assay) has recently led to the discovery of the first metabolic resistance marker in CYP450s (Mugenzi et al., 2019; Weedall et al., 2019). However, the ability of this gene *CYP325A* to confer pyrethroid resistance and the underlying molecular process remain uncharacterised.

Therefore, to fill this gap in knowledge, we investigated the role played by *CYP325A* in pyrethroid resistance in resistant populations of *An. funestus* from Cameroon, Central Africa. Up-regulation of this gene is highly associated with resistance to both type I and II pyrethroids in field populations of *An. funestus* in Cameroon. Through *in vitro* recombinant protein expression, metabolic assays, and modelling and molecular docking simulations we showed that *CYP325A* can metabolise both type I and II pyrethroids, albeit with greater efficiency against type I.

2. Materials and methods

2.1. Study sites

Blood-fed female *Anopheles* mosquitoes were collected from Mibellon (6°46′N, 11° 70′E), a rural village in Cameroon, Adamawa Region, (Fig. S1A). This region forms a transition between forested south and northern savannah of Cameroon and comprises of several water bodies such as lakes and swamplands which act as suitable breeding sites for mosquitoes (Menze et al., 2018) Major activities in this region include subsistence farming, fishing, and hunting. Menze et al. (2018) identified high use of insecticides in agriculture, mainly pyrethroids, neonicotinoids and carbamates in this region (Menze et al., 2018). Other mosquito samples used in this study are samples collected during previous studies conducted across Africa (Fig. S1B) (Ibrahim et al., 2016a, 2019; Menze et al., 2018; Riveron et al., 2015, 2016, 2017, 2018b). Field mosquitoes from four different regions of Africa with different resistant profiles were utilized, together with the susceptible laboratory strain FANG, originally from Angola, as well as the resistant laboratory strain FUMOZ originating from Mozambique. The field resistant mosquitoes were from Southern Africa: Chikwawa in Malawi (Barnes et al., 2017); East Africa: Tororo in Uganda (Okia et al., 2018); West Africa: Kpome in Benin (Tchigossou et al., 2018) and Obuasi in Ghana (Riveron et al., 2016); Central Africa: Mibellon in Cameroon (Menze et al., 2018) and Kinshasa in DRC. The pyrethroid resistance profiles of these mosquito populations have been previously established.

2.2. Mosquito collection and rearing

Blood fed, indoor resting female *An. funestus* mosquitoes were collected early in the morning, between 06:00 and 11:00 in the houses after verbal consent was obtained from household heads. Mosquitoes were collected in Mibellon in March 2018 using the Prokopack electrical aspirator (John W. Hook, Gainesville, FL, USA) and kept in netted paper cups that were stored in a cool box. Samples were transported to the insectary of Centre for Research in Infectious Disease (CRID) Yaoundé, Cameroon. Fully gravid mosquitoes, obtained after 4–5 days were induced to lay eggs using the forced egg-laying method (Morgan et al., 2010) in cups containing mineral water for hatching. After hatching, the larvae were reared to adult and mosquitoes mixed in cages (Cuamba et al., 2010; Morgan et al., 2010).

2.2.1. Species identification

All female mosquitoes used for individual ovipositing were morphologically identified as belonging to the *An. funestus* group according to the identification key of Coetzee (2020). The genomic DNA was extracted using the Livak method (Livak, 1984; Livak and Schmittgen, 2001) and a cocktail PCR assay (Koekemoer et al., 2002) was used to confirm that all females that laid eggs were *An. funestus* sensu stricto.

2.3. Insecticide resistance profile of field population of An. funestus in Mibellon

Insecticide susceptibility bioassays were conducted using 2- to 5-day-old F_1 adult female mosquitoes from pooled F_1 mosquitoes, following the WHO protocol (WHO, 2016). For each insecticide approximately 20–25 female mosquitoes per tube were exposed to either permethrin (0.75%) or deltamethrin (0.05%) impregnated papers for 30 min, 1 h and 1.5 h, and transferred to a clean holding tube immediately, supplied with 10% sugar solution, and mortality determined 24 h later. For each

test, mosquitoes exposed to untreated papers were used as controls. The assay was carried out at temperatures of 25 °C ± 2 and 80% ± 10 relative humidity.

As P450 monooxygenases have previously been involved in pyrethroid resistance in *An. funestus* (Riveron et al., 2013) their potential involvement in resistance was assessed in the Mibellon mosquito population using PBO (piperonyl butoxide), a synergist/inhibitor of P450s (Feyereisen, 2012; Menze et al., 2018). 100 female mosquitoes were pre-exposed to 4% PBO papers for 1 h and immediately exposed to 0.75% permethrin or 0.05% deltamethrin for 1 h. Mortality was assessed after 24 h and compared to the results obtained without PBO (Menze et al., 2018). Significance levels were assessed using the chi-squared test at $p < 0.05$ (McHugh, 2013).

2.4. Comparative investigation of expression profile of CYP325A Africa-wide

The expression profile of *CYP325A* was investigated by qRT-PCR using mosquitoes from six different locations in Africa, to confirm its higher overexpression in Central Africa (Cameroon and DRC) compared with East (Uganda) and southern Africa (Malawi) (Weedall et al., 2019). Primers used are listed in Table 1 in Fig. S2. Total RNA was extracted from three biological replicates (three pools of 10 females) of the mosquitoes that survived exposure following the WHO test procedures for insecticide resistance monitoring in malaria vector mosquitoes (WHO, 2016) to permethrin and DDT from Cameroon, Malawi, Uganda, Ghana, and Benin; and bendiocarb from Malawi and Ghana. For each insecticide/location a control of same replicates of unexposed females were used. The FANG susceptible strain was used as control susceptible *An. funestus* population. One microgram of the RNA was used for cDNA synthesis using SuperScript III (Invitrogen) with oligo-dT20 and RNAase H following the manufacturer's instructions. Using the standard protocol (Kwiatkowska et al., 2013; Riveron et al., 2013) for qRT-PCR, the amplification was conducted after establishing the standard curve for *CYP325A*. Relative expression and fold change of *CYP325A* for the test sample and control were established by comparisons to expression levels from FANG susceptible colony, after normalization with the housekeeping genes ribosomal protein S7 (RSP7; AFUN007153) and actin 5C (AFUN002505).

2.5. Africa-wide genetic polymorphism analysis of CYP325A

2.5.1. Polymorphism analysis of CYP325A alleles

cDNA of permethrin-resistant samples from Cameroon, Benin, Uganda, Malawi, DRC, the resistant FUMOZ laboratory colony and the susceptible FANG laboratory colony were used to assess the role of allelic variation in resistance.

The amplification was done with the cDNA from section 2.4, using Phusion Taq polymerase. Primers are provided in Table 1 of Fig. S2. The PCR products were cloned into PJET1.2 blunt end vector, miniprepped and plasmids sequenced using the above primers. The sequences were cleaned using Chromas version 2.6.2 (Joó and Clark, 2012) and BioEdit (Hall, 1999) then aligned in multiple alignments using ClustalW (Thompson et al., 2003). Population genetic parameters, including nucleotide diversity and haplotype diversity were assessed using DnaSP version 6.12.03 (Rozas et al., 2003). A haplotype network was built using the TCS program (Clement et al., 2000) and a maximum likelihood phylogenetic tree was constructed using MEGA X (Kumar et al., 2018).

In addition, to assess the potential association between polymorphisms in the promoter region and pyrethroid resistance, a 1 kb genomic fragment upstream of *CYP325A* was amplified, cloned as above, and sequenced in 19 susceptible (dead after 30 min exposure to permethrin) and 16 resistant (alive after 90 min exposure to permethrin) mosquitoes from Cameroon. The primers used are listed in Fig. S2.

2.6. Prediction of activity of CYP325A using in silico analysis

2.6.1. Homology modelling and docking

To predict the potential pyrethroid metabolising capability of *CYP325A*, models were created using MODELLER 9v25 (Fiser and Šali, 2003; Webb and Sali, 2014), using human *CYP3A4* (PDB: 1TQN) (Yano et al., 2004), which shares 25.63% identity, as a template. 20 models were generated for each sequence and the most qualitative models selected based on Errat version 2.0 (Colovos and Yeates, 1993) assessment. Ligand structures were retrieved from ZINC[15] library (https://zinc.docking.org/) (Sterling and Irwin, 2015). The 3D protein models and ligands were prepared for docking using Molegro Molecular Viewer 2.5 (http://www.clcbio.com/). To predict the pattern of interactions between the enzymes and insecticides, docking was carried out with Molegro Virtual Docker 7.0.0 (Bitencourt-Ferreira and de Azevedo, 2019), with MolScore scoring function (Eldridge et al., 1997) and active site defined as a cavity of 20 Å radius centred above the haem iron. 50 binding poses were obtained for each ligand for 1R-*cis* permethrin, (ZINC01850374), deltamethrin (ZINC01997854) α-cypermethrin (ZINC2526765), bendiocarb (ZINC02015426), and DDT (ZINC01530011), which were sorted according to hybrid $MolDock_{GRID}$ score (Korb et al., 2009) and the conformation of ligands in the active site of *CYP325A*. Figures were prepared using the PyMOL 2.4 (DeLano and Bromberg, 2004) and Molegro Molecular Viewer 7 (http://www.clcbio.com/).

2.7. Comparative sequence characterisation of An. funestus CYP325A to its orthologs

Additionally, to identify the features of *CYP325A* which could impact its activity, its coding sequence was compared to other closely related P450s. Putative substrate recognition sites 1 to 6 of *An. funestus CYP325A*, *An. gambiae CYP325A* (AGAP002208), *An. stephensi CYP325A* (ASTE004501) and *An. epiroticus CYP325A* (AEPI000241) were compared by mapping their amino acid sequences to that of *Pseudomonas putida CYP101A* (P450cam) (Ibrahim et al., 2016a; Poulos et al., 1987). The locations of amino acid differences in the sequences were mapped by identifying helices A-L and substrate recognition sites (SRS1-6) using crystal structures of CYP2 family (Gotoh, 1992), and structurally conserved regions of the were also predicted using an online tool, CYPED (http://www.cyped.uni-stuttgart.de/) (Poulos et al., 1985;

Table 1
Genetic parameters of *CYP325A* in laboratory and field population no selective sweep in *CYP325A*.

Complete sequenced fragment (1512bp)												
Sample	n	S	h	Hd	Syn	Nsyn	π	D	D*	Ka	Ks	Ka/Ks
FUMOZ	9	13	3	0.417	5	8	0.194	−1.88947 *	−2.14486 **	0.154	0.314	0.49
FANG	7	5	2	0.286	1	4	0.094	−1.48614ns	−1.56696ns	0.099	0.081	1.22
DRC	8	9	4	0.643	4	5	0.162	−1.47121 ns	−1.51047 ns	0.124	0.282	0.43
Cameroon	16	10	2	0.125	5	5	0.083	−2.18261 **	−2.98819 **	0.054	0.177	0.31
All	40	49	9	0.746	n.a	n.a	0.801	0.18277ns	−0.99808ns	0.473	1.929	0.24

n, number of sequences; S, number of polymorphic sites; Syn, Synonymous mutations; Nsyn, Non-synonymous mutations; π, nucleotide diversity; D and D* Tajima's and Fu and Li's statistics; ns, not significant; π, ka and ks are multiplied by 10^2, * = $P < 0.05$; ** = $P < 0.02$, n.a not applicable.

Šali et al., 1995; Sirim et al., 2010a).

2.8. Assessment of metabolic activity of CYP325A

2.8.1. Heterologous expression of recombinant CYP325A in E. coli and metabolic assays

A recombinant CYP325A gene was expressed for the predominant haplotypes where this gene was differentially expressed (Cameroon and DR Congo). Expression plasmids pB13:*omp*A+2-CYP325A were prepared for Cameroon-CYP325A (hereby CMR-CYP325A) and DRC-CYP325A (DRC-CYP325A). The CYP325A sequences from the susceptible colony, FANG could not be expressed because the sequences retained all three introns. The recombinant plasmids were constructed by fusing cDNA fragment from a bacterial *omp*A+2 leader sequence with its downstream ala-pro linker to the NH_2-terminus of the *CYP325A* cDNA, in frame with the P450 initiation codon, as described (Pritchard et al., 1997); and then cloned into *Nde*I- and *Eco*RI-linearised pCW-ori + vector (McLaughlin et al., 2008). Details of PCR conditions used to create this type of expression plasmid cassettes have already been described (Ibrahim et al., 2015; Riveron et al., 2013) and list of primers are provided in Fig. S2. The *E. coli JM109* cells were co-transformed with the P450 expression cassettes and a plasmid containing the *An. gambiae* cytochrome P450 reductase in pACYC-184 expression vector (pACYC-AgCPR) fused to pelB leader sequence (Pritchard et al., 1997; Willats et al., 1999). Membrane expression and preparations, measurement of P450 content, measurement of cytochrome *c* reductase activity, cytochrome b_5 expression and measurement of its content were carried out as previously described (Guengerich et al., 2009; Omura and Sato, 1964; Sato, 1964; Stevenson, Bradley J. et al., 2011). Metabolic assays were conducted as previously described (Ibrahim et al., 2015; Riveron et al., 2014a). 0.2 M Tris-HCl and NADPH regeneration components (1 mM glucose-6-phosphate, 0.25 mM $MgCl_2$, 0.1 mM NADP and 1 U/ml glucose-6-phosphate dehydrogenase) were added to the bottom of 1.5 ml tube chilled on ice. Membrane expressing recombinant CYP325A and AgCPR, and reconstituted cytochrome b_5 were added to the side of the tube and pre-incubated for 5 min at 30 °C, with shaking at 1200 rpm to activate the membrane. 20 μM of test insecticides (permethrin or deltamethrin) was added into the final volume of 0.2 ml (~2.5% v/v methanol), and reaction started by vortexing at 1200 rpm and 30 °C for 1 h. Reactions were quenched with 0.1 ml ice-cold methanol and incubated for 5 more min. Tubes were then centrifuged at 16,000 rpm and 4 °C for 15 min, and 150 μl of supernatant transferred into HPLC vials for analysis. Reactions were carried out in triplicates with experimental samples (+NADPH) and negative controls (-NADPH). 100 μl of sample was loaded onto an isocratic mobile phase (90:10 v/v methanol to water) with a flow rate of 1 ml/min, monitoring wavelength of 226 nm and peaks separated with a 250 mm C18 column (Acclaim 120, Dionex) on Agilent 1260 Infinity at 23 °C. Enzyme activity was calculated as percentage depletion (the difference in the quantity of insecticide(s) remaining in the +NADPH tubes compared with the –NADPH) and a *t*-test used to assess significance (Kim, 2015). For permethrin, deltamethrin and α-cypermethrin using the Cameroon and DRC recombinant CYP325A, steady state kinetic parameters were determined by measuring the rate reaction for 20 min at varying substrate concentrations (0–30 μM) in presence of 50 pmol recombinant CYP325A. Reactions were replicated in triplicate for both + NADPH and –NADPH at each concentration. K_m and V_{max} were established from the plot of substrate concentrations against the initial velocities and fitting of the data to the Michaelis-Menten module using the least squares non-linear regression in GraphPad Prism 6.03 Software (Swift, 1997).

2.9. Analysis of selective sweep spanning CYP325A using PoolSeq

2.9.1. Genetic diversity of CYP325A

Reads from pooled population data were aligned to the $AfunF_1$ chromosomal assembly of *Anopheles funestus* (Ghurye et al., 2019) using bwa (Li and Durbin, 2009). Variants were called at a minor allele frequency of 0.01 in Varscan (Koboldt et al., 2009) and SNPs within 20bp of indels removed using bcftools (Li et al., 2009). Variants were annotated in snpEff (Cingolani et al., 2012) and coding sequence SNP variants for *CYP325A* input to SNPGenie (Nelson et al., 2015). Non-synonymous site diversity (π_n) and synonymous diversity (π_s) were extracted from SNPGenie results per population for *CYP325A* (AFUN015966), and diversity estimates compared between populations. We compared diversity estimates at *CYP325A* with three genes *CYP9K1*, *CYP6P9a* and *CYP6P9b*, which we know to have undergone selective sweeps across Africa (Mugenzi et al., 2019; Weedall et al., 2019, 2020). Alignments were also inspected visually in IGV (Robinson et al., 2011) for a region 10,000bp up- and down-stream of the *CYP325A* to identify any structural variation and gene duplication events.

2.10. Polymorphism analysis of 1 kb putative promoter in Cameroon in relation to resistance phenotype

Assessment of the correlation of polymorphism of *CYP325A* and pyrethroid resistance was conducted by individually amplifying and direct sequencing a 5′UTR segment of the promoter region of *CYP325A,* 1061 bp upstream of the ATG codon. This was done using 19 mosquitoes dead after 30 min exposure to permethrin (susceptible) and 15 mosquitoes alive after 90 min exposure to permethrin (resistant) from Mibellon. Amplification was carried out using the following conditions: initial denaturation of one cycle at 94 °C for 3 min; followed by 35 cycles each of 95 °C for 30 s (denaturation), 60 °C for 30 s (annealing), and extension at 72 °C for 1 min; and one cycle at 72 °C for 5 min (final elongation). PCR products were cleaned individually with QIAquick® PCR Purification Kit (QIAGEN, Hilden, Germany) and cloned into pJET1.2/blunt according to manufacturer's protocol (ThermoFisher Scientific, MA, USA). These were then used to transform in *Escherichia coli* $DH_5\alpha$, plasmids miniprepped with the QIAprep Miniprep Kit (QIAGEN, Hilden, Germany). Three clones per sample were sequenced on both strands using the pJET1.2 sequencing primers. The polymorphic positions were detected through a manual analysis of sequence traces using BioEdit 7.2.5 (Hall et al., 2011) and sequence differences and multiple alignments using ClustalW, DnaSP 6.12.03 (Rozas et al., 2017) was used to define and to assess genetic parameters, such as nucleotide diversity (π), haplotype diversity and the D and D* selection estimates. A maximum likelihood tree of the haplotypes for both cDNA and genomic amplifications was constructed using MEGA 10.0.4 (Kumar et al., 1994), and a haplotype network was built using the TCS program (95% connection limit, gaps treated as a fifth state) to assess the potential connection between haplotypes and resistance phenotypes (Clement et al., 2002). The data was represented in histograms using GraphPad Prism 7.0 (Swift, 1997).

3. Results

3.1. Characterisation of the Anopheles funestus population from Mibellon

3.1.1. Mosquito identification and insecticide resistance profile

Cocktail PCR of the indoor collected F_0 females confirmed all 288 mosquitoes collected at Mibellon as *An. funestus* s.s.

The Mibellon *An. funestus* mosquitoes showed very high resistance to permethrin (mortality = 28.6% ± 4.13 for 60 min exposure and 50% ± 17.57 for 90 min) and deltamethrin (mortality = 16.8% ± 5.05 for 60 min and 52.3% ± 8.3 for 90 min) (Fig. 1A). Pre-exposure of mosquitoes to PBO restored full susceptibility to both pyrethroids (mortality = 98.8% ± 3.77 for permethrin and 96.5% ± 1.16 for deltamethrin at 60 min exposure, respectively) (Fig. 1B), suggesting the role of cytochrome P450s resistance to pyrethroids in this population.

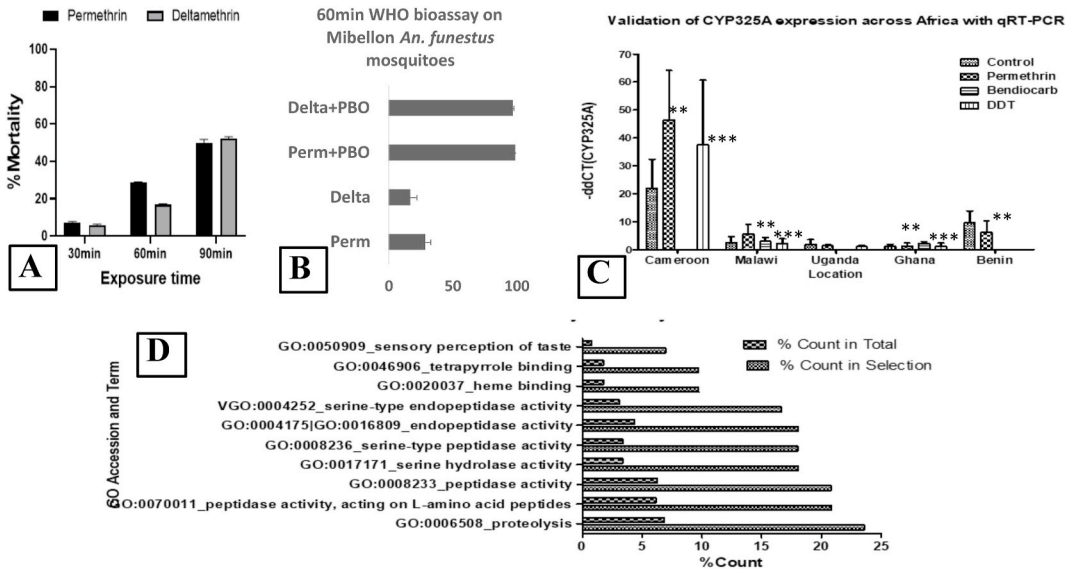

Fig. 1. Susceptibility profile of *An. funestus* mosquitoes to insecticide. A. Recorded mortalities following 30 min, 60 min and 90 min exposure of *An. funestus s.s.* from Mibellon to different insecticides **B.** Activities of PBO combined to permethrin and deltamethrin on *An. funestus* s.s. from Mibellon, Cameroon **C.** Differential expression of *CYP325A* in the *An. funestus* s.s. Mibellon population in Cameroon, measured by qRT-PCR. *p < 0.05, **p < 0.01 and ***p < 0.001, $X^2 = 14.245$. The *p*-value is 0.00016 and significant at p-value p < 0.05 **D.** Gene ontology (GO) for *CYP325A* entity similarity.

3.2. Expression profile of CYP325A

3.2.1. Pattern of expression of CYP325A across Africa

qRT-PCR confirmed the overexpression of *CYP325A* in Central Africa, Cameroon with fold-change of ~45 in permethrin resistant mosquitoes. In contrast the expression level was low in other regions of Africa, for example, southern region (Malawi), East (Uganda) and West Africa (Ghana and Benin), with fold changes <5 in line with prior RNA-Seq analyses (Mugenzi et al., 2019). Moreover, a greater over-expression of *CYP325A* was observed in Cameroonian mosquitoes that survived exposure to permethrin than in those not exposed to insecticide (control) ($p < 0.05$) (Fig. 1C).

3.2.2. Detection of transcripts presenting a similar expression pattern to CYP325A in An. funestus populations

STRAND NGS software, version 3.4 (Strand Life Sciences, Bangalore, India) was used to detect the list of entities (transcripts) exhibiting a similar expression pattern to *CYP325A* and likely to be involved in the same molecular pathway. AFUN015966 (*CYP325A*) was selected in the permethrin-resistant samples and a criteria of similarity index of >0.7 was set comparing expression in mosquitoes resistant to permethrin, resistant to DDT, control mosquitoes not exposed to insecticides in Cameroon and to the FANG susceptible strain. A total of 148 transcripts were found to have index of similarity of >0.7 with *CYP325A*. Among these, detoxification genes were detected including cytochrome P450s, glutathione S-transferases (GSTs), ABC transporters. Among P450s, *CYP6P5* had the highest similarity expression to *CYP325A* [Similarity Index (SI) = 0.8] followed by *CYP6P9b* (SI = 0.73). The GSTs included *GSTe2* (SI = 0.75) and *GSTe6* (SI = 0.74). Two transcription factors also presented a similar expression pattern to *CYP325A,* notably CCAAT/enhancer-binding protein gamma (SI = 0.78) and transcription factor Adf-1 both known to bind to the promoter and the enhancer regions of target genes. The list also includes other genes such as serine proteases (Trypsin and Chymotrypsin 2), an ABC transporter (AFUN019220) and two microRNAs (mir-279 and mir-71).

A Gene Ontology (GO) enrichment analysis of the list of the 148 similarly expressed genes to *CYP325A* revealed an over-representation of 10 GO terms (Fig. 1D) reflecting the function of those transcripts including detoxification (haem binding, tetrapyrrole binding) and serine protease activity (serine-type endopeptidase activity, serine hydrolase activity, proteolysis).

3.3. Africa-wide genetic polymorphism analysis of CYP325A

3.3.1. Polymorphism analysis of cDNA

Screening for the genetic variability of 1512 bp *CYP325A* cDNA for 9 clones for FUMOZ, 7 clones for FANG, 8 clones for DRC and 16 clones for Cameroon revealed a relatively high polymorphism in this gene (Table 1). The Cameroon samples had a reduced variation when compared to the other localities with 2 haplotypes and the lowest haplotype diversity (Hd) (Fig. 2B, Table 1) and nucleotide diversity (Fig. S3), while samples from DRC were the most polymorphic. Tajima's D was negative for all the populations but significantly so only for Cameroon and FUMOZ suggesting a recent population expansion possibly after a bottleneck or a selective sweep. This is reflected in the presence of a major clade for the Cameroon samples (which cluster separately from field sequences from resistant populations in all the other countries) in the maximum likelihood phylogenetic tree (Fig. 2A).

3.3.2. Whole genome PoolSeq analysis of selective sweep across CYP325A

Analyses of whole genome PoolSeq sequences from 12 populations across Africa revealed that diversity estimates of each site type were no different between Cameroon and other populations (Fig. S4). By contrast a very clear decrease was seen in diversity in Uganda, for *CYP9K1* and in Southern African populations and the FUMOZ resistant strain for *CYP6P9a* and *CYP6P9b*. Inspection of read alignments in IGV did not reveal any difference between Cameroon and other populations across the region inspected.

3.3.3. Polymorphism analysis of 1 kb putative promoter

An. funestus mosquitoes from Mibellon, Cameroon exposed to permethrin were used to establish the polymorphism patterns of a 1 kb promoter region upstream of the 5′-UTR of *CYP325A*. The results revealed significant differences between alive and dead mosquitoes (Table 2). Analysis of the upstream region (1 kb) showed reduced diversity in the resistant samples compared to the susceptible. This is evident in a lower number of haplotypes (3 vs 8) and polymorphic sites (13 vs 46) suggesting a possible ongoing directional selection in resistant mosquitoes, although the positive values obtained for the Tajima's D and Fu and Li statistics points towards a balancing selection. The

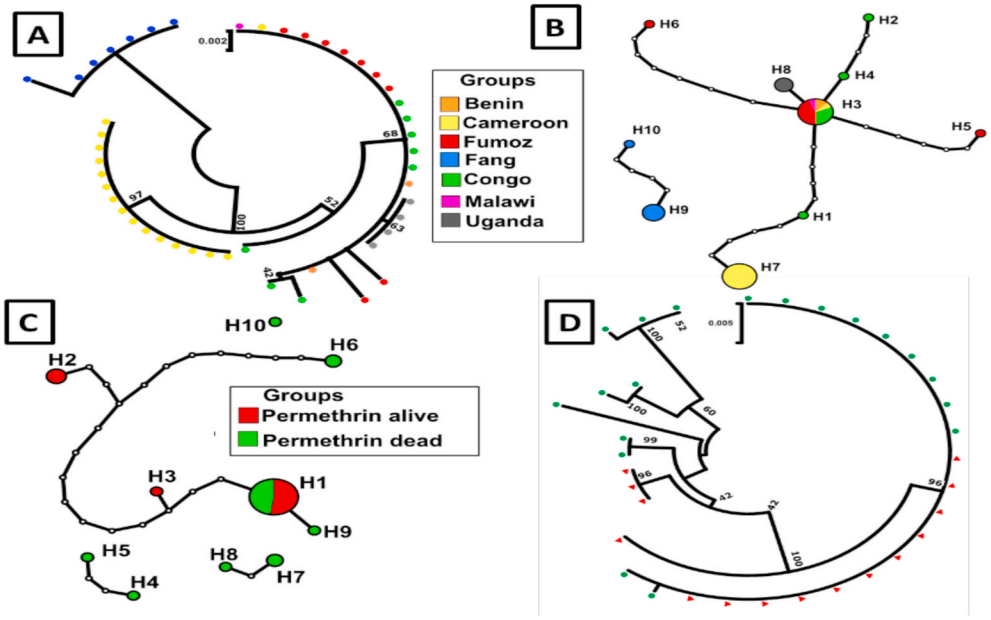

Fig. 2. Population studies of *CYP325A* coding sequences across Africaand 1kb putative promoter from Cameroon A. Phylogenetic tree for *CYP325A* cDNA across Africa. **B.** Haplotype diversity network of *CYP325A* cDNA for FANG, FUMOZ, Cameroon, Malawi, Benin, Uganda, and DRC. **C.** Haplotype diversity network analysis of 1kb putative promoter of *CYP325A* between permethrin alive and dead samples, **D.** Phylogenetic tree of 1kb putative promoter of *CYP325A* between permethrin alive and dead samples revealing a dominant haplotype being shared between the resistant and the susceptible.

Table 2
Genetic parameters of a 1 kb putative promoter of *CYP325A* upstream of ATG between permethrin alive and dead samples.

Sample	n	S	h	Hd	π	D	D*
Alive	15	13	3	0.448	0.448	0.67629 ns	1.47811 **
Dead	19	46	8	0.725	1.307	−0.09242 ns	−0.17703 ns
All	34	48	10	0.617	0.975	−0.66073 ns	−0.35501 ns

n = number of sequences; S, number of polymorphic sites; Syn, Synonymous mutations; Nsyn, Non-synonymous mutations; π, nucleotide diversity; D and D* Tajima's and Fu and Li's statistics; ns, not significant; π is multiplied by 10^2, ** = $P < 0.01$.

haplotype network (Fig. 2C) and phylogenetic tree (Fig. 2D) showed a predominance of haplotype H1 (73%) in the alive mosquitoes compared to the dead ones with a marked difference in haplotype diversity (Fig. S5C). Other haplotypes were only specific to the resistant (H2 and H3) and susceptible (H4, H5, H6, H7, and H8) (Figure S5, A and B) with susceptible haplotypes presenting the highest number of mutational steps (5 haplotypes with >20 mutational steps) to the major H1 haplotype further supporting the reduced diversity in resistant mosquitoes.

3.4. Amino acid sequence characterisation of *An. funestus CYP325A*

Comparison of *An. funestus CYP325A* to other closely related sequences revealed it is 72.8% identical to *An. gambiae CYP325A* (AGAP002208), 74.8% identical to *An. epiroticus CYP325A* (AEPI000241) and 81.9% identical to *An. stephensi CYP325A* (ASTE004501) (Fig. S6). Apart from *An. epiroticus CYP325A* (499 amino acids) and *An. gambiae CYP325A* (505 amino acids), the other two P450s are made of 503 amino acids. Sequence-to-sequence mapping reveals that the WxxxR motif, the signatory oxygen-binding pocket (AGFETS)/ proton transfer groove, the ExxR motif which stabilises the haem structural core, the cysteine pocket/haem-binding region (PFxxGxxxCxG), which forms the fifth axial ligand to the haem iron were all identical and conserved in the three different *Anopheles* sequences. Major variations which could impact the activity of *An. funestus CYP325A* compared with *An. gambiae CYP325A* were not observed in all the substrate recognition sites (SRSs) and helices except the αK helix (Ala^{371} in *An. funestus CYP325A* and Gly^{371} in *An. gambiae*) and the SRS-2 (Gly^{205} in *An. stephensi* and Cys^{205} in the others). In the meander at positions 424 and 425, amino acid variations were observed $S^{424}Q$ in *An. epiroticus* and $S^{424}A$ in *An. gambiae*.

3.5. Prediction of activity of *CYP325A* using in silico analysis

3.5.1. Homology modelling and docking

The models of *CYP325A* alleles from Cameroon and DRC were used to predict ability to metabolise insecticides. Docking simulation was carried out using permethrin, α-cypermethrin, deltamethrin, bendiocarb and DDT. The calculated binding parameters for each insecticide, demonstrating their most favourable, productive, and properly oriented poses, are given in Fig. S8.

Permethrin, deltamethrin and α-cypermethrin exhibited high scores compared to bendiocarb and DDT consistent with the resistance profile in Mibellon population, where DDT resistance has been shown to be driven by *GSTe2* (D Menze et al., 2018; Menze et al., 2018; Riveron et al., 2014b). Comparison of the different conformations of the insecticide molecules in the active site of *CYP325A* revealed the possible mechanisms through which this gene could drive pyrethroid resistance. For permethrin, the CMR_*CYP325A* model was exhibited in the correct orientation with the benzyl ring located within 3-5Å of the haem catalytic site as shown in the binding pose (Fig. 3A and Fig. 3B). These poses predict a ring hydroxylation to produce 2-hydroxypermethrin. The permethrin productive poses show two major amino acids involved, namely $Serine^{208}$ and $Serine^{207}$, with the latter forming a H-bond interactions with the ester oxygen, at 2-4Å.

For type II pyrethroids deltamethrin and α-cypermethrin, a different pattern was observed. Deltamethrin docked with the phenoxy ring above the haem and the 4'spot located within 4.5 Å from the haem iron (Fig. 3C and Fig. S9B). In this posture, the ring hydroxylation to generate 4′-hydroxydeltamethrin is possible. Also, the benzyl ring docked within 5 Å of the haem iron with the possibility of hydroxylation. Like the permethrin docking, deltamethrin and α-cypermethrin were found to dock productively in several binding modes mainly interacting with Ser^{207}, Ser^{208} and Arg^{115} with strong H-bonds and near the haem catalytic site. (Fig. 3D and Fig. S9C).

Bendiocarb docked very close (3 Å), with the aromatic ring oriented to the haem catalytic site and forms very strong H-bond interactions with the Ser^{207}, Ser^{208} and Arg^{115} in some suggestively productive poses in the proper orientation. The carbamic ester group oriented away from the haem iron (Fig. 3E and Fig. S9D).

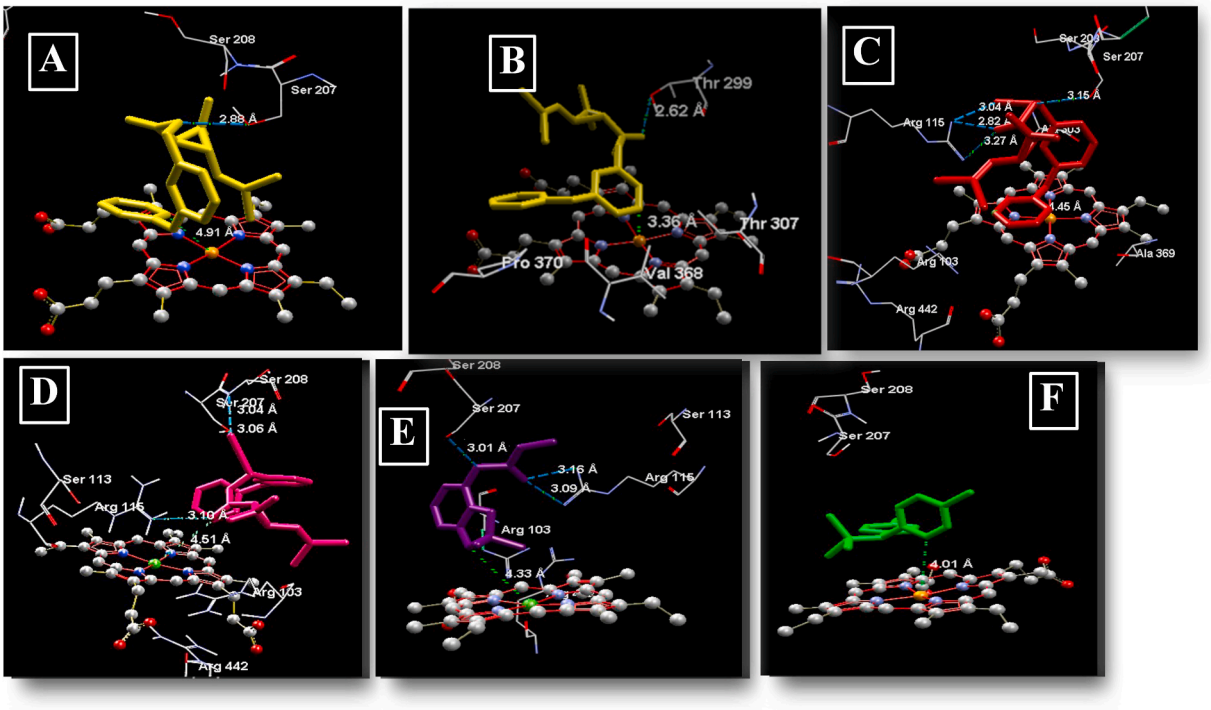

Fig. 3. Comparative *in silico* docking of (A) Permethrin_CMR, **(B)** Permethrin_DRC, **(C)** Deltamethrin_CMR, **(D)** α-Cypermethrin_CMR, **(E)** Bendiocarb_CMR and **(F)** DDT_CMR to *CYP325A* Cameroon model. Poses showing permethrin and deltamethrin in the active site of CYP325A. Permethrin (yellow) and deltamethrin (red), α-cypermethrin (pink), bendiocarb (purple) and DDT (green) is in stick format while CYP325A amino acids are in white stick format. Haem atoms are in stick format and grey/red/blue. Distance between possible sites of metabolism and haem iron is annotated in Angstrom. (For interpretation of the references to colour in this figure legend, the reader is referred to the Web version of this article.)

DDT docked in the *CYP325A* Cameroon model unproductively with the trichloromethyl group positioned approximately 7 Å away from the haem catalysis centre. No non-bonded interactions, e.g., H-bond or VDW interactions were observed between DDT and the nearby amino acids (Fig. 3F and Fig. S9E). The postures show there is a very low possibility of reductive dichlorination to produce DDE due to the distance from the haem catalysis site.

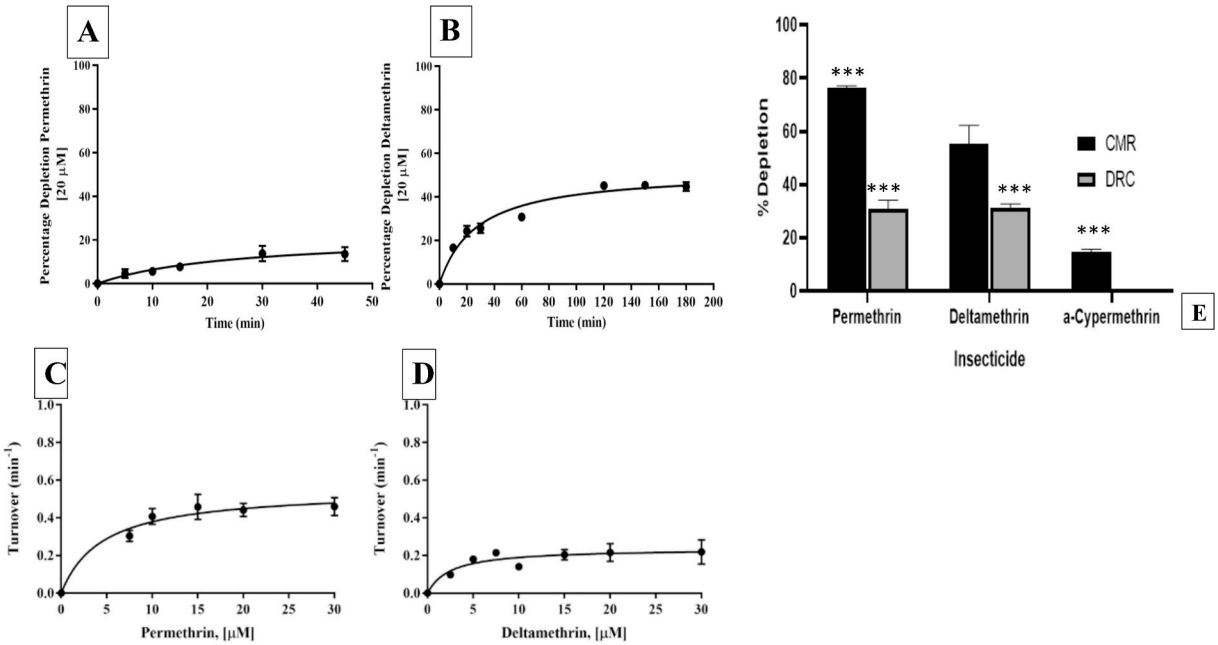

Fig. 4. *In vitro* assay results. Functional confirmation of the metabolic activity of *CYP325A* conducted for permethrin and deltamethrin using protein membranes. (A) Permethrin metabolism by recombinant CYP325A-CMR **(B)** Deltamethrin metabolism by recombinant CYP325A-CMR. Michaelis-Menten plot of permethrin and deltamethrin metabolism by recombinant *CYP325A*-CMR protein. Values are mean ± SEM of three experimental replicates compared with negative control without NADPH (-NADPH). **(C)**. Permethrin **(D)**. Deltamethrin ***$p < 0.0001$.

3.6. Assessment of metabolic activity of CYP325A

3.6.1. Protein expression pattern of CYP325A

CYP325A expressed with concentrations of 9.606 ± 0.0.71 nmol protein for Cameroon and 2.29 ± 0.40 nmol protein for DRC.

3.6.2. Validation of the role of An. funestus CYP325A in metabolism of insecticides using in vitro metabolism assays

Disappearance of 20 μM insecticides substrates was determined after 90 min of incubation with the recombinant CYP325A in the presence of cytochrome b_5 and NADPH regeneration system. CYP325A-CMR significantly metabolized permethrin with depletion of 76.5% ± 0.6 ($p < 0.0001$), deltamethrin at 55.4% ± 6.9 ($p < 0.0634$) and α-cypermethrin at 14.7% ± 1.0 ($p < 0.0001$), while CYP325A-DRC metabolized permethrin with only a depletion of 30.8% ± 3.4 ($p < 0.0001$) and deltamethrin at 31.2% ± 1.6 ($p < 0.0001$) but showed no activity towards α-cypermethrin (Fig. 4E). For the non-pyrethroid (bendiocarb and propoxur), no depletion was observed indicating lack of enzymatic activity toward carbamate insecticides. Initial analysis of reaction rates established that the CYP325A-CMR metabolized both permethrin and deltamethrin with turnovers of $K_{cat} = 0.613\ min^{-1} \pm 0.005939$ (95% CI (0.4815–0.8163)) and $K_{cat} = 0.2571\ min^{-1} \pm 0.0290$ (95% CI (0.199–0.3458)), respectively (Fig. 4A and B). Reaction follows Michaelis-Menten pattern, with a low catalytic rate; $K_{cat} = 0.613\ min^{-1} \pm 0.006$ and $K_{cat} = 0.2571\ min^{-1} \pm 0.03$ respectively, for permethrin and deltamethrin (Fig. 4C and D). Reaction speed was more than double for permethrin compared to deltamethrin. However, the affinity (K_m) for deltamethrin was double that of permethrin; $K_m = 4.597\ \mu M \pm 1.819$ and $K_m = 2.349\ \mu M \pm 1.261$, respectively. The K_m values were within the normal range of 1–50 μM, associated with substrate binding and P450 metabolism (Stevenson et al., 2012). Turnover kinetic studies determined K_m and V_{max} values of *CYP325A* showing enzyme-substrate affinity for pyrethroid however, K_{cat} values obtained for CYP325A are lower than those obtained for CYP6P9a (5.77 ± 1.48 min−1 and 5.91 ± 1.64 min−1 for permethrin and deltamethrin, respectively), CYP6P9b (6.43 ± 1.40 min−1 and 7.041 ± 1.98 min−1 with permethrin and deltamethrin, respectively), CYP6M7 (5.71 ± 1.52 min−1 for permethrin and 6.25 ± 1.67 min−1 for deltamethrin) and CYP6AA1 (K_{cat}) of 11.99 min−1 ± 2.17 and 15.65 min−1 ± 2.642, respectively for permethrin and deltamethrin) (Ibrahim et al., 2018; Riveron et al., 2014a).

Thus, the recombinant CYP325A exhibited comparable catalytic efficiency (K_{cat}/K_m) of 0.1333 $min^{-1}\mu M^{-1} \pm 0.0527$ for permethrin and 0.109 $min^{-1}\mu M^{-1} \pm 0.060$ for deltamethrin.

In this study, it was impossible to use FANG as control because all six FANG sequences obtained had retained all three introns possessed by this gene (Fig. S10).

4. Discussion

Elucidation of resistance mechanisms to insecticides in mosquito vectors of tropical diseases such as malaria is a prerequisite for better management of the growing problem of resistance to existing insecticide classes. If progress has been made in elucidating the molecular basis of pyrethroid resistance in southern African populations of *An. funestus*, little progress has been made in other African regions, most notably Central Africa. This study investigated the role of the overexpressed *CYP325A* P450 in pyrethroid resistance in *An. funestus* mosquito population in Cameroon, revealing that this gene likely contributes to resistance to types I and II pyrethroids in this region.

4.1. CYP325A over-expression is observed only in Central Africa

qRT-PCR expression patterns revealed a stark contrast in the expression pattern of *CYP325A* with high over-expression in Cameroon, Central Africa as previously reported by RNAseq (Mugenzi et al., 2019; Weedall et al., 2019) whereas other populations from other regions exhibit a low expression (Nkemngo et al., 2020). This contrasting expression profile is like that of other Africa-wide transcriptomic analyses which have consistently shown a drastic difference of expression between African regions. This is the case with the duplicated P450s *CYP6P9a* and *CYP6P9b* highly over-expressed mainly in southern Africa (Riveron et al., 2013; Weedall et al., 2019). Similarly, *GSTe2* was shown to be massively over-expressed mainly in *An. funestus* populations from West Africa, notably in Benin, whereas *CYP9K1* is predominantly overexpressed mainly in East Africa (Tchouakui et al., 2021). This contrasting expression of major resistance genes further support evidence that pyrethroid resistance has been independently selected across these regions while also highlighting the potential restriction to gene flow between populations of *An. funestus* across the continent. Such contrast in expression of metabolic resistance genes is also observed in other major malaria vectors including *An. gambiae, An. coluzzii, An. albimanus* and *An. arabiensis* (Dia et al., 2018; Gueye et al., 2020; Mackenzie-Impoinvil et al., 2019; Mitchell et al., 2012). Interestingly, the *CYP6P5* gene was shown to have the most similar expression pattern to *CYP325A* in Cameroon, where it is also overexpressed (Weedall et al., 2019). This could be linked to their potential common role in resistance as is the case in the Mibellon (Weedall et al., 2020) population. Two transcription factors CCAAT/enhancer binding protein gamma and Adf-1 also showed a high similarity in expression to *CYP325*A, a possible link between gene expression and regulation (Amador et al., 2001).

4.2. CYP325A metabolism of pyrethroids establishes its role in resistance in Central African An. funestus

Both modelling and *in vitro* studies showed that *CYP325A* alleles from Cameroon and DRC can metabolise type I pyrethroids (permethrin) and type II pyrethroids (deltamethrin). The depletion rates observed against permethrin and deltamethrin are lower than that of other P450s previously shown to metabolise pyrethroids in *An. funestus* such as *CYP6P9a* (Riveron et al., 2014a), *CYP6P9b* (Riveron et al., 2013), *CYP6M7* (Riveron et al., 2014a), *CYP9J11* (Riveron et al., 2017), *CYP6AA1* (Ibrahim et al., 2018). This level of depletion is also like that of other genes from *An. gambiae* such as *CYP6M2 and CYP6P3* found to mediate metabolic resistance to both type I and II pyrethroids (Müller et al., 2008; Wagah et al., 2021). However, the low depletion rate of *CYP325A* against alphacypermethrin suggests that it does not confer alphacypermethrin resistance. The inability of *CYP325A* to metabolise all pyrethroids is similar to previous reports that some genes could metabolise one type of pyrethroid insecticides but not the other as seen for *CYP6P4*'s ability to metabolise permethrin but not deltamethrin in *An. arabiensis* in Chad (Ibrahim et al., 2016b). The inability of *CYP325A* to metabolise efficiently α-cypermethrin in *An. funestus* mosquitoes could be an advantage for the use of LLINs impregnated with this insecticide such as Interceptor G2 as a vector control tool in the localities where *CYP325A*-based pyrethroid resistance is predominant in *An. funestus*. However, because other genes may confer alpha-cypermethrin resistance, the susceptibility of field populations to this insecticide should be monitored before making any decision. The *CYP325A* allele from DRC exhibited a significantly lower efficiency in breaking down pyrethroids than the CMR allele. This is likely due to the allelic variation ($E^{331}Q$) observed between the sequences from Cameroon and DRC. This allelic variation is due to a key mutation $E^{331}Q$ observed between Cameroon and DRC alleles. The almost fixed nature of $E^{331}Q$ mutations in Cameroon compared to their low frequency in DRC suggests this allele is under selection and will increase over time like the case of *CYP6P9a/b* in southern Africa (Weedall et al., 2019) and *GSTe2* in Benin (Riveron et al., 2014b). The mutations selected and almost fixed in the Cameroon sequences are $V^{21}L$, $R^{22}K$, $A^{29}K$ and $E^{331}Q$, however, the key mutation is at position 331 where glutamic acid (E) is replaced by glutamine (Q) in almost all the Cameroon sequences. This mutation is a major change from an acidic amino acid to a basic amino acid which could greatly

impact the physio-chemical properties of this enzyme. Even though it is not located in any substrate recognition site (SRS), it is in very close proximity to the SRS-4 and the αJ loop comprised in the proposed reductase interaction phase playing a role in substrate specificity and their electron transfer partners as part of the haem-binding core along with the αD, αE, αI, αL and αK loops (Sirim et al., 2010b). The impact of allelic variation on the metabolic efficiency of detoxification genes has previously been shown in *An. funestus* for P450s such as *CYP6P9a/b* (Ibrahim et al., 2015) and for the *GSTe2* for which a single L119F amino acid change was shown to drive DDT and pyrethroid resistance in West/central Africa. Such a role of allelic variation is also similar to the case of *CYP6A2* in *Drosophila melanogaster* for which three amino acid substitutions located close to the active site in the allele predominant in DDT-resistant flies, have been shown to confer the increasing metabolism of DDT (Feyereisen, 2012; Li et al., 2007). Further studies, such as site-directed mutagenesis could confirm the role of *CYP325A* overexpression in pyrethroid resistance and the $E^{331}Q$ mutation in the activity of *CYP325A*. Some *CYP450* genes have been established as non-metabolisers of pyrethroids even though they bind productively such as *An. gambiae CYP6Z2* for permethrin and α-cypermethrin (McLaughlin et al., 2008) and *An. arabiensis CYP6P4*. Our modelling in this study supports productive binding modes for permethrin, deltamethrin and α-cypermethrin, with possibility of binding to bendiocarb, but not DDT. However, the low similarity between *CYP325A* and the template, *CYP3A4* could have resulted in a model with lower quality, which would impact the molecular docking resolution.

4.3. Lack of strong signatures of selective sweep around CYP325A

Polymorphism analyses of the *CYP325A* full-length gene in *An. funestus* mosquitoes from across Africa revealed an overall absence of selection across this gene highlighted by the lack of a predominant resistance haplotype despite the previous observation that the $E^{331}Q$ was conferring a greater catalytic ability to the allele from Cameroon. The absence of such positive selection could suggest that the selective pressure is still relatively recent on the population from Cameroon supported by moderate resistance levels observed in Mibellon (Menze et al., 2018). The lack of selection on *CYP325A* could also suggest that this gene acts through increased expression and bioavailability similar to the highly polymorphic *CYP6M7* (Riveron et al., 2014a), and contrary to the observation made for *CYP6P9a/b* for which allelic variation drives resistance through directionally selected alleles now nearly fixed in field populations from southern Africa (Riveron et al., 2013; Weedall et al., 2019, 2020).

Furthermore, the regional comparison of the transcription profile of pyrethroid resistance in *An. funestus* cDNA across Africa and 1 kb putative promoter in permethrin susceptible (dead) and resistant (alive) mosquitoes from Mibellon, Cameroon revealed several facts. The polymorphism pattern analysis revealed a possible selection in the promoter region notably in Cameroon although further analyses are needed to confirm the extent of this selection and its impact on the cis regulation of *CYP325A*. A preliminary screening of the transcription factors binding sites in this promoter region using Alggen online software revealed the presence of binding sites for Cncc/Maf, H96, Dfd-1 and AHR/Arnt; all xenobiotic sensors previously implicated in regulation of detoxification genes like P450s (Hu et al., 2019, 2021). Further promoter activity analyses will establish the impact of these polymorphisms on the activity of *CYP325A* across Africa potentially helping to detect causative markers driving *CYP325A*-based pyrethroid resistance as done for *CYP6P9a/b* (Mugenzi et al., 2019; Weedall et al., 2019).

5. Conclusion

Knowledge of the underlying mechanisms and molecular drivers of insecticide resistance is crucial in the efficient management of insecticide resistance in malaria vectors. However, such knowledge requires understanding the molecular basis of the resistance which can then be applied by vector control programs for more effective intervention and management strategies. Here, we established that the P450 *CYP325A* is highly implicated in the resistance against the bed net insecticides permethrin and deltamethrin in the *An. funestus* mosquito population in Cameroon, Central Africa. These findings will help pave the way to detect the associated molecular markers to facilitate the design of DNA-based diagnostic tools to track this resistance in the field.

Author contributions

CSW conceived and designed the study. JDB was the academic supervisor of the study and reviewed the manuscript; ANRW performed the molecular and biochemical experiments with contributions from SSI and MOK; ANRW, SSI and AM conducted the *in vitro* assays; JH performed the Poolseq analyses and writeup, MJW provided the qRT-PCR data and handled the sequencing process at CRID, HI helped acquire pCW plasmid for the enzyme characterization work and handled the sequencing process at LSTM, LMJM contributed to the population genetics analyses, ANRW analysed the data with contributions from CSW, JH, LMJM, SSI and MOK; ANRW, SSI, JH, and CSW wrote the manuscript with contributions from all authors.

Accession numbers

CYP325A sequences- GenBank MW542209-MW542311 for the 1 kb putative promoter and cDNA. Data analysed in this study are available in public repositories (ENA archive for Cameroon PoolSeq: PRJEB24384) or available within the article and its Supplementary Information files. Further details are available from the authors upon request.

Funding

This work was supported by a Wellcome Trust Senior Research Fellowship in Biomedical Sciences to CSW (101893/Z/13/Z and 217188/Z/19/Z).

Declaration of competing interest

The authors declare no competing interests.

Acknowledgements

We thank Dr Magellan Tchouakui, Williams Tchapga, Tchoupo Micareme, Ebai Terence, Doumani Djonabaye, Mangoua Mersimine, Fotso Toguem Yvan, Dr Tresor Melachio, and Dr Daniel Nguete from CRID, for assistance in optimisation, logistics and data analyses. A special thanks to Dr Mark Paine (LSTM) for providing the pCW-ori + plasmid used in enzyme characterization in this study.

Appendix A. Supplementary data

Supplementary data to this article can be found online at https://doi.org/10.1016/j.ibmb.2021.103647.

References

Amador, A., Papaceit, M., Juan, E., 2001. Evolutionary change in the structure of the regulatory region that drives tissue and temporally regulated expression of alcohol dehydrogenase gene in Drosophila funebris. Insect Mol. Biol. 10 (3), 237–247.

Antonio-Nkondjio, C., Defo-Talom, B., Tagne-Fotso, R., Tene-Fossog, B., Ndo, C., Lehman, L.G., Awono-Ambene, P., 2012. High mosquito burden and malaria transmission in a district of the city of Douala, Cameroon. BMC Infect. Dis. 12 (1), 275.

Antonio-Nkondjio, C., Fossog, B.T., Ndo, C., Djantio, B.M., Togouet, S.Z., Awono-Ambene, P., Ranson, H., 2011. Anopheles gambiae distribution and insecticide resistance in the cities of Douala and Yaoundé (Cameroon): influence of urban agriculture and pollution. Malar. J. 10 (1), 154.

Barnes, K.G., Irving, H., Chiumia, M., Mzilahowa, T., Coleman, M., Hemingway, J., Wondji, C.S., 2017. Restriction to gene flow is associated with changes in the molecular basis of pyrethroid resistance in the malaria vector Anopheles funestus. Proc. Natl. Acad. Sci. Unit. States Am. 114 (2), 286–291.
Bitencourt-Ferreira, G., de Azevedo, W.F., 2019. Molegro Virtual Docker for Docking *Docking Screens For Drug Discovery*. Springer, pp. 149–167.
Chiu, T.-L., Wen, Z., Rupasinghe, S.G., Schuler, M.A., 2008. Comparative molecular modeling of Anopheles gambiae CYP6Z1, a mosquito P450 capable of metabolizing DDT. Proc. Natl. Acad. Sci. Unit. States Am. 105 (26), 8855–8860.
Cingolani, P., Platts, A., Wang, L.L., Coon, M., Nguyen, T., Wang, L., Ruden, D.M., 2012. A program for annotating and predicting the effects of single nucleotide polymorphisms, SnpEff: SNPs in the genome of Drosophila melanogaster strain w1118; iso-2; iso-3. Fly 6 (2), 80–92.
Clement, M., Posada, D., Crandall, K.A., 2000. TCS: a computer program to estimate gene genealogies. Mol. Ecol. 9 (10), 1657–1659.
Clement, M., Snell, Q., Walker, P., Posada, D., Crandall, K., 2002. TCS: estimating gene genealogies. Paper presented at the Parallel and Distributed Processing Symposium. International 3, 0184-0184.
Coetzee, M., 2020. Key to the females of Afrotropical Anopheles mosquitoes (Diptera: Culicidae). Malar. J. 19 (1), 1–20.
Colovos, C., Yeates, T.O., 1993. Verification of protein structures: patterns of nonbonded atomic interactions. Protein Sci. 2 (9), 1511–1519.
Cuamba, N., Morgan, J.C., Irving, H., Steven, A., Wondji, C.S., 2010. High level of pyrethroid resistance in an Anopheles funestus population of the Chokwe District in Mozambique. PloS One 5 (6), e11010.
D Menze, B., Wondji, M.J., Tchapga, W., Tchoupo, M., Riveron, J.M., Wondji, C.S., 2018. Bionomics and insecticides resistance profiling of malaria vectors at a selected site for experimental hut trials in central Cameroon. Malar. J. 17 (1), 1–10.
DeLano, W.L., Bromberg, S., 2004. PyMOL User's Guide. DeLano Scientific LLC, p. 629.
Dia, A.K., Guèye, O.K., Niang, E.A., Diédhiou, S.M., Sy, M.D., Konaté, A., Faye, O., 2018. Insecticide resistance in Anopheles arabiensis populations from Dakar and its suburbs: role of target site and metabolic resistance mechanisms. Malar. J. 17 (1), 1–9.
Diengou, N.H., Cumber, S.N., Nkfusai, C.N., Mbinyui, M.S., Viyoff, V.Z., Bede, F., Judith, A.-K., 2020. Factors associated with the uptake of intermittent preventive treatment of malaria in pregnancy in the Bamenda health districts, Cameroon. The Pan African Medical Journal 35.
Djouaka, R., Riveron, J.M., Yessoufou, A., Tchigossou, G., Akoton, R., Irving, H., Tamò, M., 2016. Multiple insecticide resistance in an infected population of the malaria vector Anopheles funestus in Benin. Parasites Vectors 9 (1), 1–12.
Eldridge, M.D., Murray, C.W., Auton, T.R., Paolini, G.V., Mee, R.P., 1997. Empirical scoring functions: I. The development of a fast empirical scoring function to estimate the binding affinity of ligands in receptor complexes. J. Comput. Aided Mol. Des. 11 (5), 425–445.
Feyereisen, R., 2012. Insect CYP Genes and P450 Enzymes *Insect Molecular Biology and Biochemistry*. Elsevier, pp. 236–316.
Fiser, A., Šali, A., 2003. Modeller: Generation and Refinement of Homology-Based Protein Structure Models Methods in Enzymology, vol. 374. Elsevier, pp. 461–491.
Ghurye, J., Koren, S., Small, S.T., Redmond, S., Howell, P., Phillippy, A.M., Besansky, N. J., 2019. A chromosome-scale assembly of the major African malaria vector Anopheles funestus. GigaScience 8 (6), giz063.
Gotoh, O., 1992. Substrate recognition sites in cytochrome P450 family 2 (CYP2) proteins inferred from comparative analyses of amino acid and coding nucleotide sequences. J. Biol. Chem. 267 (1), 83–90.
Guengerich, F.P., Martin, M.V., Sohl, C.D., Cheng, Q., 2009. Measurement of cytochrome P450 and NADPH–cytochrome P450 reductase. Nat. Protoc. 4 (9), 1245–1251.
Gueye, O., Tchouakui, M., Dia, A.K., Faye, M.B., Ahmed, A.A., Wondji, M.J., Konaté, L., 2020. Insecticide resistance profiling of Anopheles coluzzii and Anopheles gambiae populations in the southern Senegal: role of target sites and metabolic resistance mechanisms. Genes 11 (12), 1403.
Hall, T., Biosciences, I., Carlsbad, C., 2011. BioEdit: an important software for molecular biology. GERF Bull. Biosci. 2 (1), 60–61.
Hall, T.A., 1999. BioEdit: a User-Friendly Biological Sequence Alignment Editor and Analysis Program for Windows 95/98/NT. In: Paper Presented at the Nucleic Acids Symposium Series.
Hemingway, J., 2014. The role of vector control in stopping the transmission of malaria: threats and opportunities. Phil. Trans. Biol. Sci. 369 (1645), 20130431.
Hu, B., Huang, H., Hu, S., Ren, M., Wei, Q., Tian, X., Reddy Palli, S., 2021. Changes in both trans-and cis-regulatory elements mediate insecticide resistance in a lepidopteron pest, Spodoptera exigua. PLoS Genet. 17 (3), e1009403.
Hu, B., Huang, H., Wei, Q., Ren, M., Mburu, D.K., Tian, X., Su, J., 2019. Transcription factors CncC/Maf and AhR/ARNT coordinately regulate the expression of multiple GSTs conferring resistance to chlorpyrifos and cypermethrin in Spodoptera exigua. Pest Manag. Sci. 75 (7), 2009–2019.
Ibrahim, S.S., Amvongo-Adjia, N., Wondji, M.J., Irving, H., Riveron, J.M., Wondji, C.S., 2018. Pyrethroid resistance in the major malaria vector Anopheles funestus is exacerbated by overexpression and overactivity of the P450 CYP6AA1 across Africa. Genes 9 (3), 140.
Ibrahim, S.S., Mukhtar, M.M., Datti, J.A., Irving, H., Kusimo, M.O., Tchapga, W., Wondji, C.S., 2019. Temporal escalation of Pyrethroid Resistance in the major malaria vector Anopheles coluzzii from Sahelo-Sudanian Region of northern Nigeria. Sci. Rep. 9 (1), 7395. https://doi.org/10.1038/s41598-019-43634-4.
Ibrahim, S.S., Ndula, M., Riveron, J.M., Irving, H., Wondji, C.S., 2016a. The P450 CYP 6Z1 confers carbamate/pyrethroid cross-resistance in a major African malaria vector beside a novel carbamate-insensitive N485I acetylcholinesterase-1 mutation. Mol. Ecol. 25 (14), 3436–3452.
Ibrahim, S.S., Riveron, J.M., Bibby, J., Irving, H., Yunta, C., Paine, M.J., Wondji, C.S., 2015. Allelic variation of cytochrome P450s drives resistance to bednet insecticides in a major malaria vector. PLoS Genet. 11 (10), e1005618.
Ibrahim, S.S., Riveron, J.M., Stott, R., Irving, H., Wondji, C.S., 2016b. The cytochrome P450 CYP6P4 is responsible for the high pyrethroid resistance in knockdown resistance-free Anopheles arabiensis. Insect Biochem. Mol. Biol. 68, 23–32.
Joó, B., Clark, M.A., 2012. Lattice QCD on GPU clusters, using the QUDA library and the Chroma software system. Int. J. High Perform. Comput. Appl. 26 (4), 386–398.
Kim, T.K., 2015. T test as a parametric statistic. Korean journal of anesthesiology 68 (6), 540.
Koboldt, D.C., Chen, K., Wylie, T., Larson, D.E., McLellan, M.D., Mardis, E.R., Ding, L., 2009. VarScan: variant detection in massively parallel sequencing of individual and pooled samples. Bioinformatics 25 (17), 2283–2285.
Koekemoer, L., Kamau, L., Hunt, R., Coetzee, M., 2002. A cocktail polymerase chain reaction assay to identify members of the Anopheles funestus (Diptera: Culicidae) group. Am. J. Trop. Med. Hyg. 66 (6), 804–811.
Korb, O., Stutzle, T., Exner, T.E., 2009. Empirical scoring functions for advanced protein− ligand docking with PLANTS. J. Chem. Inf. Model. 49 (1), 84–96.
Kumar, S., Stecher, G., Li, M., Knyaz, C., Tamura, K., 2018. MEGA X: molecular evolutionary genetics analysis across computing platforms. Mol. Biol. Evol. 35 (6), 1547–1549.
Kumar, S., Tamura, K., Nei, M., 1994. MEGA: molecular evolutionary genetics analysis software for microcomputers. Bioinformatics 10 (2), 189–191.
Kwiatkowska, R.M., Platt, N., Poupardin, R., Irving, H., Dabire, R.K., Mitchell, S., Wondji, C.S., 2013. Dissecting the mechanisms responsible for the multiple insecticide resistance phenotype in Anopheles gambiae ss, M form, from Vallee du Kou, Burkina Faso. Gene 519 (1), 98–106.
Li, H., Durbin, R., 2009. Fast and accurate short read alignment with Burrows–Wheeler transform. Bioinformatics 25 (14), 1754–1760.
Li, H., Handsaker, B., Wysoker, A., Fennell, T., Ruan, J., Homer, N., Durbin, R., 2009. The sequence alignment/map format and SAMtools. Bioinformatics 25 (16), 2078–2079.
Li, X., Schuler, M.A., Berenbaum, M.R., 2007. Molecular mechanisms of metabolic resistance to synthetic and natural xenobiotics. Annu. Rev. Entomol. 52, 231–253.
Livak, K.J., 1984. Organization and mapping of a sequence on the Drosophila melanogaster X and Y chromosomes that is transcribed during spermatogenesis. Genetics 107 (4), 611–634.
Livak, K.J., Schmittgen, T.D., 2001. Analysis of relative gene expression data using real-time quantitative PCR and the 2− ΔΔCT method. methods 25 (4), 402–408.
Mackenzie-Impoinvil, L., Weedall, G.D., Lol, J.C., Pinto, J., Vizcaino, L., Dzuris, N., Lenhart, A., 2019. Contrasting patterns of gene expression indicate differing pyrethroid resistance mechanisms across the range of the New World malaria vector Anopheles albimanus. PloS One 14 (1), e0210586.
McHugh, M.L., 2013. The chi-square test of independence. Biochem. Med. 23 (2), 143–149.
McLaughlin, L., Niazi, U., Bibby, J., David, J.P., Vontas, J., Hemingway, J., Paine, M., 2008. Characterization of inhibitors and substrates of Anopheles gambiae CYP6Z2. Insect Mol. Biol. 17 (2), 125–135.
Mendis, K., Rietveld, A., Warsame, M., Bosman, A., Greenwood, B., Wernsdorfer, W.H., 2009. From malaria control to eradication: the WHO perspective. Trop. Med. Int. Health 14 (7), 802–809.
Menze, B.D., Wondji, M.J., Tchapga, W., Tchoupo, M., Riveron, J.M., Wondji, C.S., 2018. Bionomics and insecticides resistance profiling of malaria vectors at a selected site for experimental hut trials in central Cameroon. Malar. J. 17 (1), 1–10.
Mitchell, S.N., Stevenson, B.J., Müller, P., Wilding, C.S., Egyir-Yawson, A., Field, S.G., Donnelly, M.J., 2012. Identification and validation of a gene causing cross-resistance between insecticide classes in Anopheles gambiae from Ghana. Proc. Natl. Acad. Sci. Unit. States Am. 109 (16), 6147–6152.
Morgan, J.C., Irving, H., Okedi, L.M., Steven, A., Wondji, C.S., 2010. Pyrethroid resistance in an Anopheles funestus population from Uganda. PloS One 5 (7), e11872.
Moyes, C.L., Lees, R.S., Yunta, C., Walker, K.J., Hemmings, K., Oladepo, F., Ismail, H.M., 2020. Evaluating the Evidence from Molecular Structure and Population Studies for Cross-Resistance to the Pyrethroids Used in Malaria Vector Control.
Mugenzi, L.M., Menze, B.D., Tchouakui, M., Wondji, M.J., Irving, H., Tchoupo, M., Wondji, C.S., 2019. Cis-regulatory CYP6P9b P450 variants associated with loss of insecticide-treated bed net efficacy against Anopheles funestus. Nat. Commun. 10 (1), 1–11.
Müller, P., Warr, E., Stevenson, B.J., Pignatelli, P.M., Morgan, J.C., Steven, A., Hemingway, J., 2008. Field-caught permethrin-resistant Anopheles gambiae overexpress CYP6P3, a P450 that metabolises pyrethroids. PLoS Genet. 4 (11), e1000286.
Nelson, C.W., Moncla, L.H., Hughes, A.L., 2015. SNPGenie: estimating evolutionary parameters to detect natural selection using pooled next-generation sequencing data. Bioinformatics 31 (22), 3709–3711.
Nikou, D., Ranson, H., Hemingway, J., 2003. An adult-specific CYP6 P450 gene is overexpressed in a pyrethroid-resistant strain of the malaria vector, Anopheles gambiae. Gene 318, 91–102.
Nkemngo, F.N., Mugenzi, L.M., Terence, E., Niang, A., Wondji, M.J., Tchoupo, M., Ntabi, J.D., 2020. Elevated Plasmodium sporozoite infection and multiple insecticide resistance in the principal malaria vectors Anopheles funestus and Anopheles gambiae in a forested locality close to the Yaoundé airport, Cameroon. Wellcome Open Research 5.
Okia, M., Hoel, D.F., Kirunda, J., Rwakimari, J.B., Mpeka, B., Ambayo, D., Govere, J., 2018. Insecticide resistance status of the malaria mosquitoes: Anopheles gambiae and Anopheles funestus in eastern and northern Uganda. Malar. J. 17 (1), 1–12.

Omura, T., Sato, R., 1964. The carbon monoxide-binding pigment of liver microsomes: I. Evidence for its hemoprotein nature. J. Biol. Chem. 239 (7), 2370–2378.
Poulos, T.L., Finzel, B., Gunsalus, I., Wagner, G.C., Kraut, J., 1985. The 2.6-A crystal structure of Pseudomonas putida cytochrome P-450. J. Biol. Chem. 260 (30), 16122–16130.
Poulos, T.L., Finzel, B.C., Howard, A.J., 1987. High-resolution crystal structure of cytochrome P450cam. J. Mol. Biol. 195 (3), 687–700.
Pritchard, M.P., Ossetian, R., Li, D.N., Henderson, C.J., Burchell, B., Wolf, C.R., Friedberg, T., 1997. A general strategy for the expression of recombinant human cytochrome P450s inEscherichia coliUsing bacterial signal peptides: expression of CYP3A4, CYP2A6, and CYP2E1. Arch. Biochem. Biophys. 345 (2), 342–354.
Riveron, J.M., Chiumia, M., Menze, B.D., Barnes, K.G., Irving, H., Ibrahim, S.S., Wondji, C.S., 2015. Rise of multiple insecticide resistance in Anopheles funestus in Malawi: a major concern for malaria vector control. Malar. J. 14 (1), 344.
Riveron, J.M., Ibrahim, S.S., Chanda, E., Mzilahowa, T., Cuamba, N., Irving, H., Wondji, C.S., 2014a. The highly polymorphic CYP6M7 cytochrome P450 gene partners with the directionally selected CYP6P9a and CYP6P9b genes to expand the pyrethroid resistance front in the malaria vector Anopheles funestus in Africa. BMC Genom. 15 (1), 817.
Riveron, J.M., Ibrahim, S.S., Mulamba, C., Djouaka, R., Irving, H., Wondji, M.J., Wondji, C.S., 2017. Genome-wide transcription and functional analyses reveal heterogeneous molecular mechanisms driving pyrethroids resistance in the major malaria vector Anopheles funestus across Africa. G3: Genes, Genomes, Genetics 7 (6), 1819–1832.
Riveron, J.M., Irving, H., Ndula, M., Barnes, K.G., Ibrahim, S.S., Paine, M.J., Wondji, C.S., 2013. Directionally selected cytochrome P450 alleles are driving the spread of pyrethroid resistance in the major malaria vector Anopheles funestus. Proc. Natl. Acad. Sci. Unit. States Am. 110 (1), 252–257.
Riveron, J.M., Osae, M., Egyir-Yawson, A., Irving, H., Ibrahim, S.S., Wondji, C.S., 2016. Multiple insecticide resistance in the major malaria vector Anopheles funestus in southern Ghana: implications for malaria control. Parasites Vectors 9 (1), 504.
Riveron, J.M., Tchouakui, M., Mugenzi, L., Menze, B.D., Chiang, M.-C., Wondji, C.S., 2018a. Insecticide Resistance in Malaria Vectors: an Update at a Global Scale *Towards Malaria Elimination-A Leap Forward*. IntechOpen.
Riveron, J.M., Watsenga, F., Irving, H., Irish, S.R., Wondji, C.S., 2018b. High Plasmodium infection rate and reduced bed net efficacy in multiple insecticide-resistant malaria vectors in Kinshasa, Democratic Republic of Congo. J. Infect. Dis. 217 (2), 320–328.
Riveron, J.M., Yunta, C., Ibrahim, S.S., Djouaka, R., Irving, H., Menze, B.D., Albert, A., 2014b. A single mutation in the GSTe2 gene allows tracking of metabolically based insecticide resistance in a major malaria vector. Genome Biol. 15 (2), R27.
Robinson, J., Thorvaldsdottir, H., Winckler, W., Guttman, M., Lander, E., 2011. Etz G, Mesirov JP, Integrative genomics viewer. Nat. Biotechnol. 29, 24–26.
Rozas, J., Ferrer-Mata, A., Sánchez-DelBarrio, J.C., Guirao-Rico, S., Librado, P., Ramos-Onsins, S.E., Sánchez-Gracia, A., 2017. DnaSP 6: DNA sequence polymorphism analysis of large data sets. Mol. Biol. Evol. 34 (12), 3299–3302.
Rozas, J., Sánchez-DelBarrio, J.C., Messeguer, X., Rozas, R., 2003. DnaSP, DNA polymorphism analyses by the coalescent and other methods. Bioinformatics 19 (18), 2496–2497.
Šali, A., Potterton, L., Yuan, F., van Vlijmen, H., Karplus, M., 1995. Evaluation of comparative protein modeling by MODELLER. Proteins: Structure, Function, and Bioinformatics 23 (3), 318–326.
Sato, T.O.a.R., 1964. The carbon monoxide-binding pigment of liver microsomes. J. Biol. Chem. 239 (7).
Sirim, D., Widmann, M., Wagner, F., Pleiss, J., 2010a. Prediction and analysis of the modular structure of cytochrome P450 monooxygenases. BMC Struct. Biol. 10 (1), 34.
Sirim, D., Widmann, M., Wagner, F., Pleiss, J., 2010b. Prediction and analysis of the modular structure of cytochrome P450 monooxygenases. BMC Struct. Biol. 10 (1), 1–12.
Sterling, T., Irwin, J.J., 2015. ZINC 15–ligand discovery for everyone. J. Chem. Inf. Model. 55 (11), 2324–2337.
Stevenson, B., Bibby, J., Pignatelli, P., Muangnoicharoen, S., O'Neill, P.M., Lian, L.-Y., Hemingway, J., 2011. Cytochrome P450 6M2 from the malaria vector Anopheles gambiae metabolizes pyrethroids: sequential metabolism of deltamethrin revealed. Insect Biochem. Mol. Biol. 41 (7), 492–502.
Stevenson, B.J., Bibby, J., Pignatelli, P., Muangnoicharoen, S., O'Neill, P.M., Lian, L.-Y., Hemingway, J., 2011. Cytochrome P450 6M2 from the malaria vector Anopheles gambiae metabolizes pyrethroids: sequential metabolism of deltamethrin revealed. Insect Biochem. Mol. Biol. 41 (7), 492–502.
Stevenson, B.J., Bibby, J., Pignatelli, P., Muangnoicharoen, S., O'Neill, P.M., Lian, L.-Y., Paine, M.J.I., 2011. Cytochrome P450 6M2 from the malaria vector Anopheles gambiae metabolizes pyrethroids: sequential metabolism of deltamethrin revealed. Insect Biochem. Mol. Biol. 41 (7), 492–502. https://doi.org/10.1016/j.ibmb.2011.02.003.
Stevenson, B.J., Pignatelli, P., Nikou, D., Paine, M.J., 2012. Pinpointing P450s associated with pyrethroid metabolism in the dengue vector, Aedes aegypti: developing new tools to combat insecticide resistance. PLoS Neglected Trop. Dis. 6 (3), e1595.
Swift, M.L., 1997. GraphPad prism, data analysis, and scientific graphing. J. Chem. Inf. Comput. Sci. 37 (2), 411–412.
Tchigossou, G., Djouaka, R., Akoton, R., Riveron, J.M., Irving, H., Atoyebi, S., Wondji, C.S., 2018. Molecular basis of permethrin and DDT resistance in an Anopheles funestus population from Benin. Parasites Vectors 11 (1), 1–13.
Tchouakui, M., Mugenzi, L.M., D Menze, B., Khaukha, J.N., Tchapga, W., Tchoupo, M., Wondji, C.S., 2021. Pyrethroid resistance aggravation in Ugandan malaria vectors is reducing bednet efficacy. Pathogens 10 (4), 415.
Tchuinkam, T., Nyih-Kong, B., Fopa, F., Simard, F., Antonio-Nkondjio, C., Awono-Ambene, H.-P., Mpoame, M., 2015. Distribution of Plasmodium falciparum gametocytes and malaria-attributable fraction of fever episodes along an altitudinal transect in Western Cameroon. Malar. J. 14 (1), 96.
Thompson, J.D., Gibson, T.J., Higgins, D.G., 2003. Multiple sequence alignment using ClustalW and ClustalX. Current protocols in bioinformatics (1), 2.3. 1-32.3. 22.
Tonye, S.G.M., Kouambeng, C., Wounang, R., Vounatsou, P., 2018. Challenges of DHS and MIS to capture the entire pattern of malaria parasite risk and intervention effects in countries with different ecological zones: the case of Cameroon. Malar. J. 17 (1), 156.
Wagah, M.G., Korlević, P., Clarkson, C., Miles, A., Lawniczak, M.K., Makunin, A., 2021. Genetic variation at the Cyp6m2 putative insecticide resistance locus in Anopheles gambiae and Anopheles coluzzii. Malar. J. 20 (1), 1–13.
Webb, B., Sali, A., 2014. Protein Structure Modeling with MODELLER *Protein Structure Prediction*. Springer, pp. 1–15.
Weedall, G.D., Mugenzi, L.M., Menze, B.D., Tchouakui, M., Ibrahim, S.S., Amvongo-Adjia, N., Djouaka, R., 2019. A cytochrome P450 allele confers pyrethroid resistance on a major African malaria vector, reducing insecticide-treated bednet efficacy. Sci. Transl. Med. 11 (484).
Weedall, G.D., Riveron, J.M., Hearn, J., Irving, H., Kamdem, C., Fouet, C., Wondji, C.S., 2020. An Africa-wide genomic evolution of insecticide resistance in the malaria vector Anopheles funestus involves selective sweeps, copy number variations, gene conversion and transposons. PLoS Genet. 16 (6), e1008822.
WHO, 2016. Test Procedures for Insecticide Resistance Monitoring in Malaria Vector Mosquitoes.
WHO, 2020. World Malaria Report 2020: 20 Years of Global Progress and Challenges.
Willats, W.G., Gilmartin, P.M., Mikkelsen, J.D., Knox, J.P., 1999. Cell wall antibodies without immunization: generation and use of de-esterified homogalacturonan block-specific antibodies from a naive phage display library. Plant J. 18 (1), 57–65.
Wondji, C.S., Morgan, J., Coetzee, M., Hunt, R.H., Steen, K., Black, W.C., Ranson, H., 2007. Mapping a quantitative trait locus (QTL) conferring pyrethroid resistance in the African malaria vector Anopheles funestus. BMC Genom. 8 (1), 1–14.
Yano, J.K., Wester, M.R., Schoch, G.A., Griffin, K.J., Stout, C.D., Johnson, E.F., 2004. The structure of human microsomal cytochrome P450 3A4 determined by X-ray crystallography to 2.05-Å resolution. J. Biol. Chem. 279 (37), 38091–38094.